

8. Soil Mechanics

*James K. Mitchell,^{a†} W. David Carrier, III,^b Nicholas C. Costes,^c
William N. Houston,^a Ronald F. Scott,^d and H. John Hovland^e*

The objectives of the soil mechanics experiment were to determine the physical characteristics and mechanical properties of the lunar soil at the surface and subsurface and the variations in lateral directions and to relate this knowledge to the interpretation of lunar history and processes. Data obtained on the lunar surface in conjunction with observations of returned samples of lunar soil are used to determine in-place density and porosity profiles and to determine strength characteristics on local and regional scales.

The soil mechanics experiment on the Apollo 17 mission to the Taurus-Littrow area of the Moon was passive and involved no apparatus or crew time unique to the experiment. The preliminary analyses and interpretations presented in this report have been deduced from studies of extravehicular activity (EVA) transcripts and kinescopes, mission photographs, data on the lunar roving vehicle (LRV) performance, debriefings, and limited examination of returned lunar samples by the Lunar Sample Preliminary Examination Team (LSPET).

SUMMARY OF PREVIOUS RESULTS

The mechanical properties of lunar soil as deduced through the Apollo 15 mission were summarized by Mitchell et al. (ref. 8-1). The Apollo 16 results agreed generally with those of earlier missions and also provided more specific quantitative information on density and strength and their variability than was available previously. Even though lunar and terrestrial soils differ greatly in mineralogical composition, lunar

soil behavior is similar to that of terrestrial soils of comparable gradation (silty fine sand). Particle-size distribution, particle shape, and relative density (ref. 8-2) control behavior.

Soil porosity, density, and strength vary locally and with depth. Absolute densities may range from approximately 1.0 to 2.0 g/cm³, and values > 1.5 g/cm³ are probable at depths > 10 to 20 cm. The relative density of the soil near the surface is extremely variable but is generally quite high (> 80 percent) below a depth of 10 to 20 cm. Although local (meter scale) variations in density and porosity exist, Houston et al. (ref. 8-3) and Mitchell et al. (ref. 8-4) have shown that the mean porosity at each of the Apollo sites from footprint analysis is approximately the same for the upper few centimeters of soil. Analysis by Costes (ref. 8-5) of vehicle tracks at the same Apollo sites and at the Mare Imbrium site of the Soviet Luna 17 yields higher average porosity values at crater rims and other soft spots than for firm soil located in intercrater areas. The soil on crater rims and on slopes appears to be more variable and, on the average, less dense and weaker than does soil in intercrater plains areas.

Relative density (or porosity) is probably the most important single variable controlling strength, with most probable values of cohesion in the range of 0.1 to 1.0 kN/m² and friction angle in the range of 30° to 50°. The higher values are associated with higher relative densities.

DATA SOURCES

Soil mechanics data were derived from crew commentary and debriefings, television, lunar surface photographs, performance data and observations of interactions between soil and the LRV, drive-tube and deep drill samples, and sample characteristics as determined by the LSPET.

^aUniversity of California at Berkeley.

^bNASA Lyndon B. Johnson Space Center.

^cNASA Marshall Space Flight Center.

^dCalifornia Institute of Technology.

^ePacific Gas and Electric Company.

[†]Principal Investigator.

Information from these data sources has been used in a manner similar to that from previous Apollo missions to deduce qualitative and semiquantitative information about soil properties. A statistical study of footprint and LRV track depths has been used as a basis for quantitative analysis of near-surface soil porosity. Premission orbital photographs and surface photographs have indicated a number of boulder tracks on the steep slopes of the North Massif and South Massif. These tracks have been analyzed by using the method of Hovland and Mitchell (ref. 8-6). Additional quantitative estimates have been based on LRV track depths and other specific observations as noted later in this section.

RESULTS AND INTERPRETATIONS

General Soil Characteristics at the Taurus-Littrow Site

Soil cover is present at all points visited in the Taurus-Littrow landing area. The surface is a similar color (gray and gray-brown) to that at the other Apollo sites, although lighter soil layers were encountered at shallow depths in some areas and orange-colored soil was exposed in a limited zone on the rim of Shorty Crater (station 4). Surface textures range from smooth areas almost free of rock fragments through patterned ground to areas heavily concentrated with larger rocks and fragments. Variability in soil properties is evident locally. Qualitative indications of this variability on a meter scale are provided in figures 8-1 to 8-3.

Soil behavior during landing, walking, driving, and sampling was comparable to that observed during previous missions. Dust was readily kicked up under foot and by the LRV, tended to adhere to any surface with which it came in contact, and inhibited normal operations on several occasions.

As readily apparent from the study of lunar surface photographs and from crew commentary, disturbed areas on the lunar surface appear darker than undisturbed areas, as has been the case at the previous landing sites. Subsequent crew observations of the landing sites from lunar orbit indicated that the disturbed areas were lighter than the undisturbed areas. This difference in appearance could indicate that the apparent changes in surface color caused by disturbance result from texture-related changes in albedo that influence the appearance when viewed

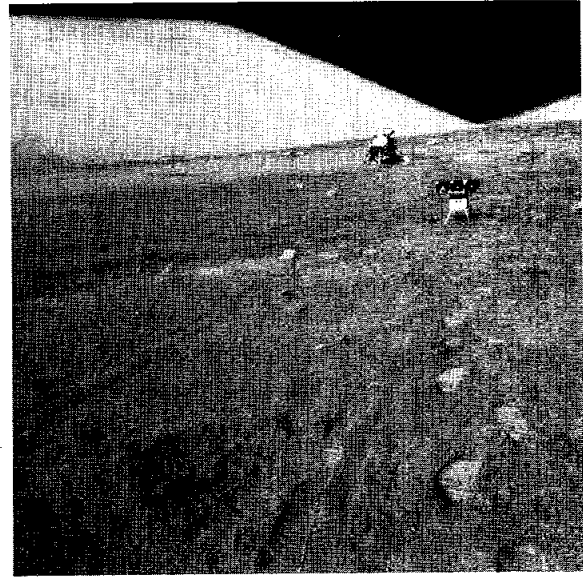


FIGURE 8-1.—Variable soil conditions in the vicinity of the surface electrical properties (SEP) experiment as evidenced by variable depths of LRV tracks and footprints (AS17-141-21517).



FIGURE 8-2.—Variable soil conditions in the light mantle at station 3 as evidenced by color differences (AS17-138-21148).

from different positions and at different Sun angles rather than from real color changes as a result of the exposure of new material. Alternatively, the different appearance might result from differences in scale between viewing from the surface and from orbit.

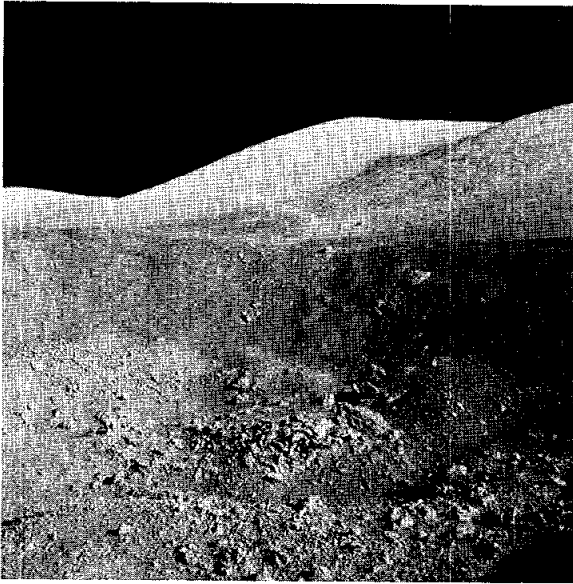


FIGURE 8-3.—Variable soil conditions inside Shorty Crater (station 4) as evidenced by different surface textures and slopes (AS17-137-21001).

Soil Observations During Lunar Module Descent and Landing

Both the postmission descent trajectory data and the crew comments indicate that the Apollo 17 descent was fairly rapid with vertical velocities of approximately 1 to 1.5 m/sec at altitudes of 60 to 70 m above the lunar surface, slowing to somewhat less than 1 m/sec at an altitude of approximately 15 to 20 m. The descent was accompanied by a fairly constant forward velocity of approximately 0.7 m/sec in the final 20 m of descent. Thus, the lunar module (LM) came in on an oblique trajectory similar to that of Apollo 14 (fig. 8-4). Previous analyses and mission results have shown that this kind of trajectory causes least disturbance of the lunar surface material during landing. In contrast, vertical descents, such as that of the Apollo 15 LM, generate substantial amounts of erosion. Blowing dust was first observed at a height of approximately 20 m above the lunar surface but caused no visibility difficulties during the final descent; in fact, the surface remained clearly visible all the way to contact.

The descent engine was shut down approximately 1 sec after contact was indicated, and the LM dropped to the lunar surface while maintaining some forward velocity. The crew noted that the rear (-Z)

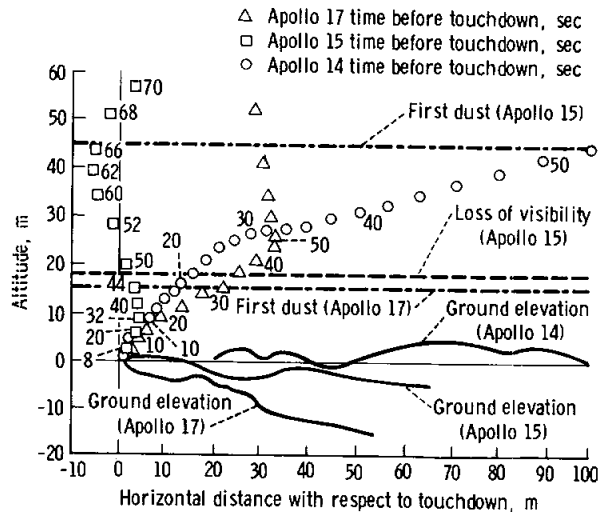


FIGURE 8-4.—Descent trajectories for the Apollo 14, 15, and 17 missions.

footpad probably hit the lunar surface first and that the primary shock absorber may have stroked slightly. Photographs (e.g., AS17-134-20388) show some crumpling of the Mylar insulation on the lower portion of the leg, indicating a possible stroking of 1 or 2 cm. This crumpling did not happen on any of the previous missions. From the photographs, no crushing of or damage to the footpad can be observed.

As in the other landings, the descent engine exhaust swept the lunar surface in the vicinity of the landing site. Compared to adjacent areas, there were relatively fewer small rock fragments and soil clumps beneath the LM, although rocks 10 cm in diameter and larger remained. The crew observed that there were clear indications of the interaction of the descent propulsion system exhaust gas with the lunar surface to a distance of approximately 50 m from the LM.

From the crew's comments during sampling, the lack of blowing dust during the final stages of the descent does not appear to be caused by soil properties different from those experienced in prior landings. As noted in the subsequent sections, the grain-size distribution, cohesion, and density of the soil around the LM are similar to those previously established for lunar soil. This similarity tends to confirm previous conclusions that the amount of blowing dust during a landing is directly related to the descent trajectory and descent rate.

Grain-Size Distribution and Soil Composition

At the time this report was prepared, the LSPET had determined the complete grain-size distribution of 15 samples and the distribution of a small aliquot of the black soil taken from the bottom of the double core-tube sample taken at station 4. The results are shown in figure 8-5. These gradations are generally similar to those observed at previous landing sites. The band of 11 samples in figure 8-5 is slightly coarser in the coarse fractions than the composite distribution band for Apollo 11, 12, 14, and 15 (ref. 8-7), primarily because of the excess particles in the fraction that is > 10 mm. This observation was also noted for some of the Apollo 16 soils (ref. 8-4) and was attributed to the recent addition of coarse fragments that had not yet been worked into the soil matrix from the South Ray Crater event. Sample 71060 was taken at station 1 from beneath a slight overhang of a rock, and the crew observed that there were chips in the soil. The distribution for sample 74240, the gray soil found next to the orange soil, was changed considerably when the total sample was included.

Despite the similarity of the grain-size distributions of the samples from various stations, the LSPET has found that the composition of the soil is highly variable in terms of proportions of basalt, breccia, mineral fragments, glass, and agglutinates. The soils from the massif stations appear to be derived from breccias, whereas much of the dark mantle on the plains was probably derived from basalts. The orange soil at station 4 is unique and is composed almost entirely of orange glass.

A knowledge of particle composition is important for the interpretation of data from many lunar experiments because, at the same relative density, soils consisting of coherent particles are stronger and conduct heat and seismic signals better than soils composed of friable particles.

Core Samples

Drive Tubes.—Data on the drive-tube samples are summarized in table 8-I, and the sampling at station 6 is shown in figure 8-6. The bulk densities of the samples in the drive tubes as a function of depth in the lunar surface are presented in figure 8-7. In all instances, the density of the soil in the lower tube is greater than that in the upper tube; that is, density

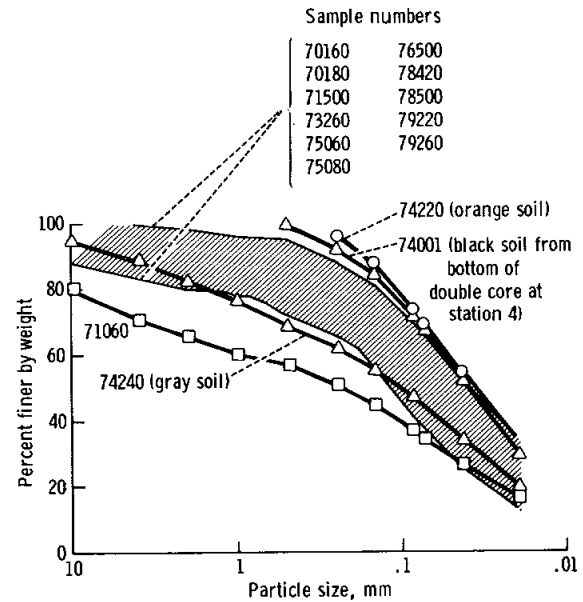


FIGURE 8-5.—Grain-size distribution curves for several Apollo 17 samples.

increases with depth, an observation consistent with findings at the Apollo 15 and 16 sites (fig. 8-7). However, the Apollo 17 core-tube densities (with the exception of the double core at station 4) are much more uniform with depth than were the Apollo 15 and 16 core-tube samples. The Apollo 17 core-tube densities tend to be higher near the surface and slightly lower below a depth of 20 to 30 cm than do the average densities for the Apollo 15 and 16 drive-tube samples.

The high core recovery percentages at stations 4 and 6 and at the LM are comparable to those of the Apollo 15 and 16 samples for which the same type of core tube was used. The lower core recovery percentages at stations 3 and 9 indicate that the returned bulk densities will have to be corrected for sample compression.

Densities in the double core from the rim of Shorty Crater at station 4 (2.03 to 2.29 g/cm³) are distinctly higher than heretofore observed for any lunar samples. The upper tube contains orange-red soil with fine-grained black soil in the lower part. Black soil is exposed at the top and bottom ends of the lower tube. The orange soil, which is composed almost entirely of glass particles, is unusually compact and exhibits a high cohesion. A trench excavated into the material illustrates the high cohesion in the

TABLE 8-I.—Preliminary Data on Apollo 17 Drive-Tube Samples

Station	Serial no.	Sample no.	Sample weight, g	Sample length, ^a cm	Bulk density, g/cm ³	Tube depth (pushed), cm	Total depth (pushed and driven), cm	No. of hammer blows	Core recovery, percent
3	2031	73002	^b 429	21.8	^c 1.60 ± 0.10	?	70.6 ± 5	≥ 9	82 ± 2
	^d 2046	73001	^b 809	^e 34.9					
4	2035	74002	^b 910	33.3	2.04	?	^{f,g} 71 ± 2	≥ 28	96 ± 3
	2044	74001	1071.4	34.9					
6	2048	76001	711.6	34.5	^e 1.57	16.2 ± 0.5	37.1 ± 0.5	^h 5 or 6	93 ± 2
9	2037	79002	409.4	19.4	^e 1.67	?	^g 71 ± 2	< 19	76 ± 2
	2050	79001	743.3	ⁱ 31.9	ⁱ 1.74				
LM	2052	70012	^j 434.8	^j 18.4	1.77	^h 28 ± 3	^h 28 ± 3	0	97 ± 10

^aDetermined from X-radiographs, except as noted.

^bSample weights are ± 4 g; better accuracy will be possible when tubes are removed from stretch cans.

^cCorrected for voids.

^dCore sample vacuum container.

^eAssumed length.

^fCamera failure; photographs were blank.

^gEstimated from kinescopes.

^hCrew estimate.

ⁱEither 41 cm³ of sample fell out of the top of the tube or the keeper compressed the top of the sample. The former is considered the more likely explanation; thus, density has been calculated accordingly.

^jApproximately 114 cm³ fell out of the bottom of the tube after it was placed in the sample collection bag because of a loose cap.

form of a tendency of the material to break into chunks (fig. 8-8).

The number of hammer blows (table 8-I), as indicated by the kinescopes, required to drive the core tube at station 4 was not exceptionally high compared to the driving resistance encountered on earlier missions, indicating that the porosity was not significantly less (or the relative density higher) at this location than had been previously encountered. Thus, the much higher bulk density is most likely caused by a higher specific gravity of the individual particles. Whereas the maximum reported value of specific gravity is 3.2 for an Apollo 15 sample (ref. 8-2), the soil in the lower half of the double core may have a value as high as 4. The black soil in the double core is composed primarily of crystalline droplets, olivine phenocrysts, a trace of glass, and 25-percent ilmenite that has a specific gravity of 4.7. The LSPET has found that the black material is the first lunar soil studied thus far that contains no agglutinates.

Drill Stems.—The deep core was drilled to a depth of 3.05 ± 0.01 m at a point approximately 40 m north of the Apollo lunar surface experiment package (ALSEP) central station. Core recovery was 95 to 97 percent, and preliminary data on the eight drill-stem sections are given in table 8-II.

Unfortunately, the top of the soil column in the top three drill-stem sections, which were returned as a unit, moved approximately 15 cm, causing some loosening and disturbance. However, because the initial sample length is known, it is possible to estimate the initial average density for the top three drill-stem sections to be 1.99 ± 0.05 g/cm³, as shown in table 8-II.

The bulk density as a function of depth in the lunar surface for the drill-stem samples is shown in figure 8-9. Values for the Apollo 15 and 16 deep drill-stem samples are shown for comparison. Because the core recovery was nearly 100 percent, the measured bulk densities should be quite close to the in situ values.

All the bulk densities are high; that of the second drill stem (2.11 g/cm³) is remarkably so. The X-radiographs indicated this section to be quite gravelly, and dissection by the LSPET has confirmed this. This zone may be related to the hard layer encountered in the LM area at the end of EVA-3 where a single core-tube sample was obtained. The fourth through the seventh drill stems all have essentially the same density; the X-radiographs show uniformity as well.

The absolute densities at the Apollo 17 drill site

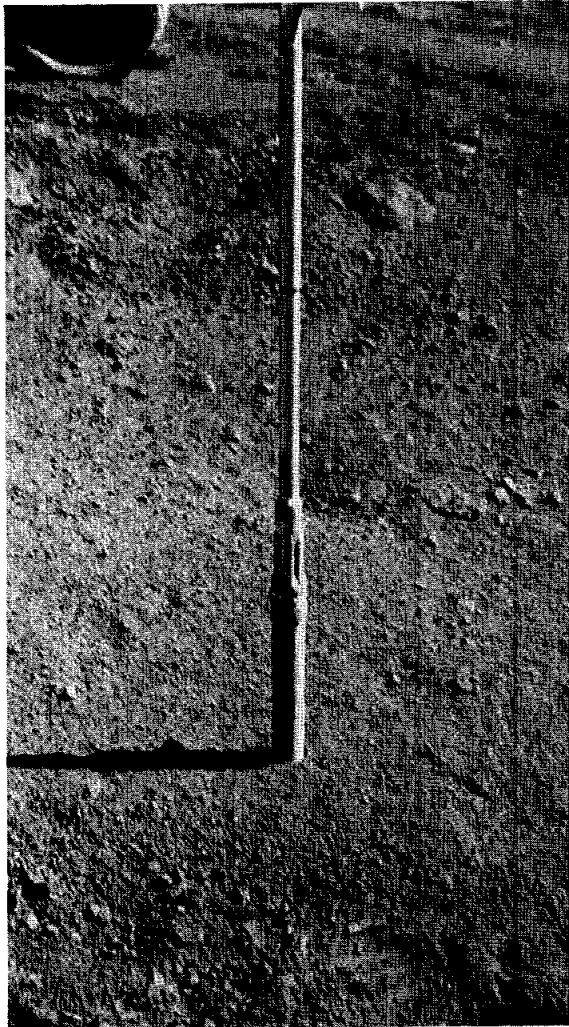


FIGURE 8-6.—Single drive tube at station 6. The drive tube has just been pushed to a depth of approximately 16 cm. A special orientation mark is visible above and to the right of the numeral 8 on the tube. This is the only drive tube from Apollo 17 that has been positively oriented in the lunar surface. After this photograph was taken, the drive tube was hammered to a final depth of 37 cm (AS17-146-22291).

are generally higher than those measured at the Apollo 15 and 16 drill sites, and the distribution of densities as a function of depth suggests a depositional history entirely different from either of the previous two sites. The average drill rate of the first Apollo 17 heat flow borestem was approximately 70 cm/min, indicating that the relative density at the the Apollo 17 site is considerably higher than that at Apollo 16 site. If the later borestem design of Apollo

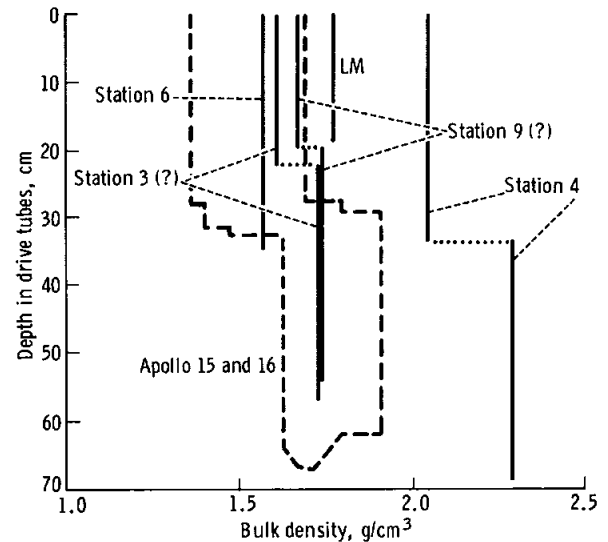


FIGURE 8-7.—Bulk density as a function of depth in the lunar surface for drive-tube samples.



FIGURE 8-8.—Trench excavated into orange soil on rim of Shorty Crater at station 4. The chunky texture reflects the high cohesion of this soil (AS17-137-20989).

16 and 17 had been available, the predicted drill rate at the Apollo 15 site would have been the same or slightly less than that measured at the Apollo 17 site, indicating that although the absolute densities in the Apollo 15 drill stem were less than those of Apollo 17, the relative densities were generally the same or higher. This indication implies a significantly different soil composition. Even though the relative densities at the Apollo 17 drill sites were indicated to

TABLE 8-II.—Preliminary Data on Apollo 17 Drill-Stem Sections

Drill-stem serial no.	Sample no.	Returned sample weight, ^a g	Returned sample length, ^b cm	Returned bulk density, ^c g/cm ³	Original sample length, ^d cm	Original bulk density, ^c g/cm ³	Drill-stem depth, cm	Core recovery, percent
061	70009	143.3	25 ± 2	1.76 ± 0.14	^e 10 ± 2	} 1.99 ± 0.05	} 305 ± 1	95 to 97
067	70008	260.9	^f 38	2.11	39.9			
063	70007	179.4	^g 34 ± 2	1.62 ± 0.10	39.9			
065	70006	234.2	39.9	1.80	39.9			
069	70005	240.6	39.9	1.85	39.9			
066	70004	238.8	39.9	1.84	39.9			
062	70003	237.8	39.9	1.83	39.9			
070	70002	207.7	} ^h 42.0	1.74	42.5			
179 (bit)	70001	29.8						

^aTotal weight is 1772.5.

^bDetermined by X-radiography.

^cBased on a sample diameter of 2.04 cm.

^dTotal length is 292 ± 2.

^eCore-tube rammer-jammer was inserted to a depth of 30 ± 2 cm before drill stem was withdrawn from soil.

^fApproximately 2-cm void at top of stem.

^gApproximately 6-cm void at top of stem.

^hNominal length is 42.5 cm; 0.5 cm fell out of bottom of drill stem on lunar surface.

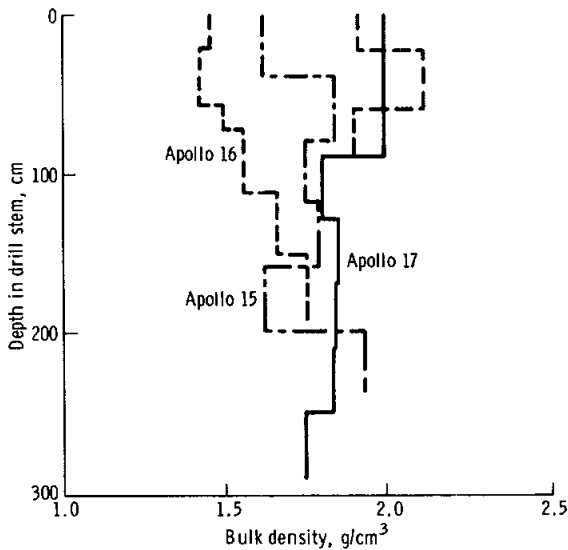


FIGURE 8-9.—Bulk density as a function of depth in the lunar surface for drill-stem samples.

not uncommon for the lunar surface and that the soil at the Apollo 16 site may have been anomalously soft. Softer soil conditions near the surface are also indicated for the Apollo 16 site by the porosity as determined by analysis of footprint depths and LRV tracks (ref. 8-1).

After extraction of the drill stem, the neutron flux probe was inserted to a depth of 2.1 m (length of probe) in the vacated hole. Before insertion of the probe, it was noted that the hole was intact and flared at the top. No resistance to insertion of the probe was encountered, except at approximately one-third the depth where a slight obstruction was noted. This resistance may have coincided with the location of the gravel layer. There was no noticeable resistance to withdrawal of the neutron flux probe at the end of EVA-3, at which time it had been in the ground for 49 hr. This suggests that there was no caving or squeezing of the soil under the increased shear stresses caused by the presence of the hole, in agreement with premission predictions.

A stability analysis of the open drill hole provides lower bound estimates of the soil strength parameters as shown by Mitchell et al. (ref. 8-8). In that report, the horizontal scale in figure 7-24 is in error. A corrected plot of the relationship between soil cohesion and friction angle and the depth to the bottom of the elastic zone in an open borehole is given in

be generally quite high, the observed drill rates were quite variable and reflected hard and soft layers at depth.

After the easy drilling experiences of Apollo 16, it was assumed that the hard drilling encountered at Apollo 15 was exceptional. On the basis of three data points, it must now be concluded that hard drilling is

figure 8-10. Below the depth corresponding to any given combination of friction angle and cohesion, a plastic zone should develop, and there should be soil yielding that would lead to closure of the hole by inward squeezing of the soil.

If no yielding of the soil developed to a depth corresponding to the length of the neutron flux probe (and little could have occurred because the probe diameter is only slightly less than the hole diameter), then the required strength parameters are as indicated by the vertical line in figure 8-10 at a depth of 2.1 m. Even for high friction angles ($> 50^\circ$), a soil cohesion exceeding 1.0 kN/m^2 is required. Strength parameters of this magnitude are likely only for conditions of high relative density and would be consistent with the hard drilling discussed previously. High strength is not required for the full depth of the hole. Stability can be maintained for conditions of strength increasing with depth to satisfy figure 8-10 at any depth.

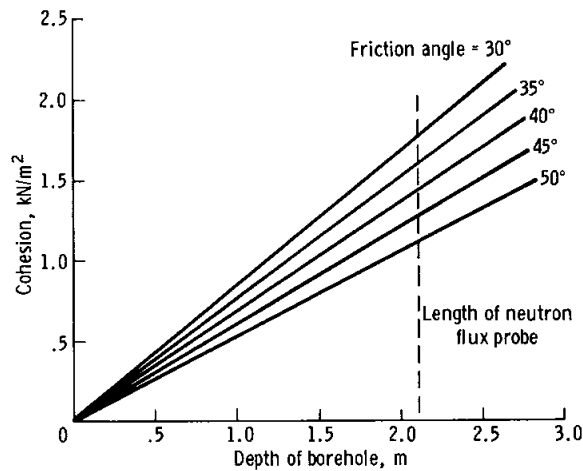


FIGURE 8-10.—Depth to bottom of the elastic zone in an open borehole as a function of soil strength parameters.

Although the open holes remaining after extraction of the drill stem suggest quite high strengths for depths of approximately 2 m at both the Apollo 16 and 17 sites, strengths of this magnitude are not commonly encountered at shallow depths as indicated by the values determined by penetrometer testing at the Apollo 16 site (ref. 8-1).

Boulder Tracks

More than 300 tracks made by boulders rolling, bouncing, and skidding down lunar slopes were identified by Grolier et al. (ref. 8-9) in the Lunar Orbiter photographs. The Apollo 17 mission provided the first opportunity for a close study of these interesting features because many tracks can be seen on the Taurus-Littrow hills. Unfortunately, prints of the 500-mm lunar surface photographs, which permit the most detailed study of the tracks, were not available to the soil mechanics team during the preparation of this report. Hence, the analyses, based mainly on 60-mm and premission orbital photographs, are tentative, and the results are subject to subsequent refinement. In a qualitative sense, boulder tracks serve as exploratory trenches and can provide information about regolith thickness and history, and the relative sharpness of track features provides some indication of soil movement after track formation.

Quantitative analysis of boulder tracks, from which information can be derived relating to soil strength and density, is possible. Studies of this type have been reported by Filice (ref. 8-10), Eggleston et al. (ref. 8-11), Moore (ref. 8-12), Moore et al. (ref. 8-13), and Hovland and Mitchell (ref. 8-6) for boulder tracks found in Lunar Orbiter photographs. The method in reference 8-6 is used here. An oblique closeup view of a larger boulder and its associated track visited at station 6 on the south slope of the

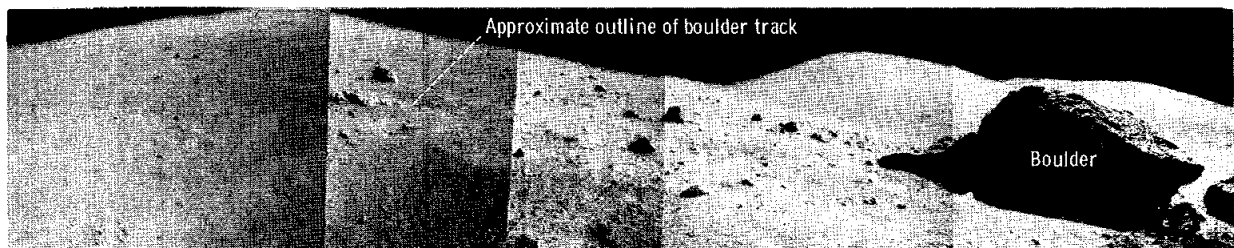


FIGURE 8-11.—Partial panorama at station 6 showing a large boulder and the track down which it rolled (AS17-141-21582, 21584, 21586, 21590, and 21594).

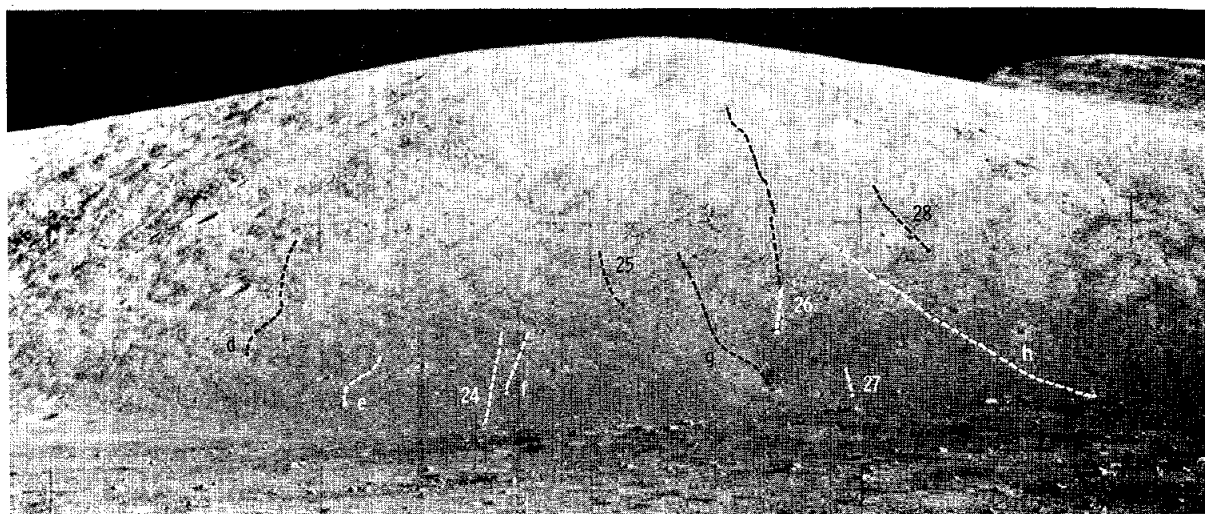
North Massif during EVA-3 is shown in figure 8-11.

Several tracks were located on the premission orbital photographs of the East Massif and the

Sculptured Hills; their locations are indicated in figure 8-12. Several tracks on the South Massif are identified in figure 8-13. Additional tracks on the



FIGURE 8-12.—Locations of boulder tracks on the East Massif and on the Sculptured Hills. For tracks identified by a letter, a definite causative boulder could be located; for tracks identified by a number, only the most probable causative boulder could be located.



----- Boulder tracks

FIGURE 8-15.—Boulder tracks on the North Massif as seen from the LM (track identifications are the same as for fig. 8-12) (AS17-147-22502).

and is used with a bearing capacity equation adapted to the case of a rolling sphere. The resulting relationships between soil friction angle, slope angle, and track-width-to-boulder-diameter ratio are shown in figure 8-16. A soil density of 1.6 g/cm^3 and a cohesion of 1 kN/m^2 were assumed. This value of cohesion is near the upper end of the range of cohesion values determined for the lunar soil thus far (refs. 8-1 and 8-4). The effect of an overestimation in cohesion by as much as a factor of 10 will lead to an underestimation of friction angle of only 1° to 2° , however. An estimate of the variations in friction angle that are likely to result from errors in a measurement of track depth and width and in boulder size has been made (ref. 8-6). The analysis indicated that friction could differ by as much as $\pm 2^\circ$ because of measurement errors.

The frequency distribution of the soil friction angles derived from the boulder track data is shown in figure 8-17 and is generally compatible with the soil gradations, densities, and porosities found at other locations on the Moon. Although the range is similar to that determined by other means (refs. 8-1 and 8-4), the most frequent values are somewhat less than would be expected because tracks of the size analyzed must involve considerably greater soil depths than for the other determinations. This difference may reflect limitations in the analysis.

Thus, the variability indicated by figure 8-17 is considered more reliable than the absolute values of friction angle.

Surface Soil Porosity Deduced from Footprint Analysis

Previously developed methods (refs. 8-3 and 8-4) have been used to extend the statistical analysis of lunar soil porosity as deduced from footprint depths to include the Apollo 17 site. The curve correlating footprint depth with average porosity and relative density of the upper few centimeters of the lunar surface, based on results of model test and theoretical analyses (ref. 8-14), is shown in figure 8-18.

A total of 144 different footprints from the Apollo 17 photographs were analyzed, and the results are summarized in table 8-IV. A histogram showing all data for Apollo 17 is presented in figure 8-19. Also summarized in table 8-IV are results for previous Apollo missions. For the Apollo 17 site, only three footprints on crater rims were analyzed. This sample size is too small to characterize crater rims statistically; thus, the values shown in table 8-IV are essentially applicable only to intercrater areas.

The data in table 8-IV show that neither the intercrater average porosity (43.4 percent) nor the standard deviation (2.4) differ significantly from the

TABLE 8-III.--Apollo 17 Boulder Tracks

Location	Reference	Track no. *	Slope angle, deg	Track length, km	Track width, w, m	Boulder diameter, D, m	$\frac{w}{D}$	Track depth, m	Friction angle, deg
East Massif	Fig. 8-12	1	23	1.3	13	17	0.76	3.0	40
		2	26	.6	10	10	1.00	5.0	30
		3	26	.6	8	15	.53	1.1	49
		4	26	.5	5	6	.83	1.3	35
		5	26	.9	12	12	1.00	6.0	30
		6	26	.7	10	16	.62	1.7	46
		a	26	1.3	9	11	.82	2.4	37
		b	26	1.7	8	10	.80	2.0	37
Sculptured Hills	Fig. 8-12	7?	25	1.3	26?	—	—	—	—
		8?	25	1.4	26?	—	—	—	—
South Massif	Fig. 8-13	9	27	0.9	10	13	0.77	2.4	39
		10	27	.9	11	16	.69	2.2	43
		11	27	2.5	10	13	.77	2.2	39
		12	27	.5	8	11	.73	1.8	41
		13	25	.4	11	15	.73	2.4	42
		14	25	.6	14	14	1.00	7.0	30
		15	25	1.4	12	12	1.00	6.0	30
	Fig. 8-14	c	25	.8	16	20	.80	4.0	39
		16	25	≈ .1	1.5	—	—	—	—
		17	25	≈ .2	3.0?	3.0	1.00	1.5	—
		18	25	≈ .05	1.8	2.1	.86	0.5	27
		19	25	≈ .3	5.0	—	—	—	—
		20	25	≈ .1	3.0?	3.0	1.00	1.5	—
		21	25	≈ .3	4.5	—	—	—	—
22	25	≈ .3	6.0	—	—	—	—		
23	25	≈ .2	3.0	2.0?	—	—	—		
North Massif	Fig. 8-15	24	26	≈ .5	7	—	—	—	—
		25	26	≈ .5	8	8	1.00	4.0	29
		26	26	≈ 1.8	10	18?	—	—	—
		27	24	≈ .1	3.6	4.5	.80	0.9	35
		28	24	≈ .7	6	8	.75	1.4	39
		d	24	≈ .9	8	10	.80	2.0	38
		e	24	≈ .4	7	9	.78	1.7	38
		f	26	≈ .4	6	6	1.00	3.0	28
		g	24	≈ 1.0	7	8	.88	2.1	33
h	23	≈ 2.0	8.5	12	.71	1.7	41		

*For tracks identified by a letter, a definite causative boulder could be located; for tracks identified by a number, only the most probable causative boulder could be located.

average values for previous Apollo sites. The Apollo 16 average (45.0 percent) is slightly higher. The statistical parameters for Apollo 17 also compare closely with both the weighted average values for all Apollo sites (44.0 percent and 2.75) and the unweighted values (43.5 percent and 2.55). The unweighted values were obtained by computing a simple arithmetic average of the averages for each site without regard to the number of observations at any

one site. Conversely, the weighted average porosity (44.0 percent) is weighted heavily in favor of Apollo 16 where an unusually large number of footprint observations was possible. Thus, the unweighted values (43.5 percent and 2.55) probably represent a better estimate for a randomly selected location on the lunar surface.

No distinguishable difference in porosity was found between the Apollo 17 traverse stations and

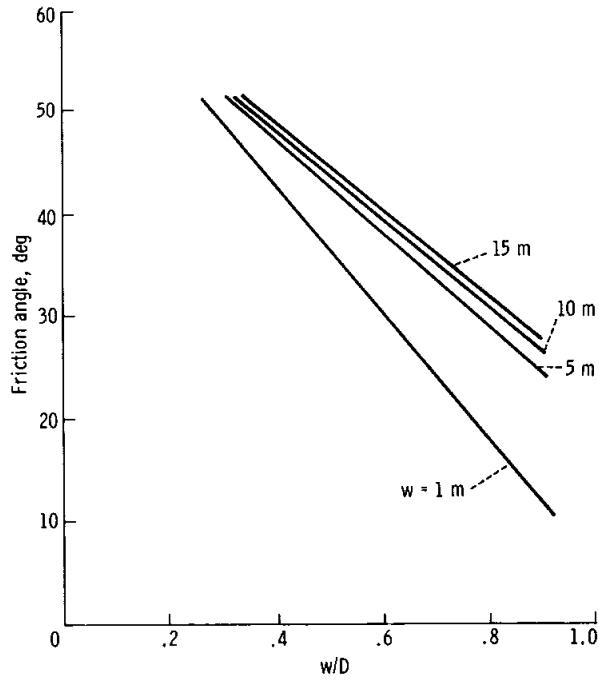
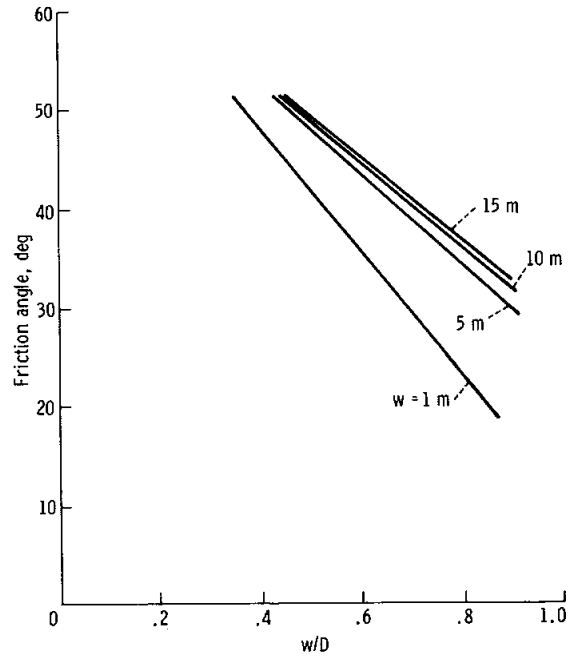
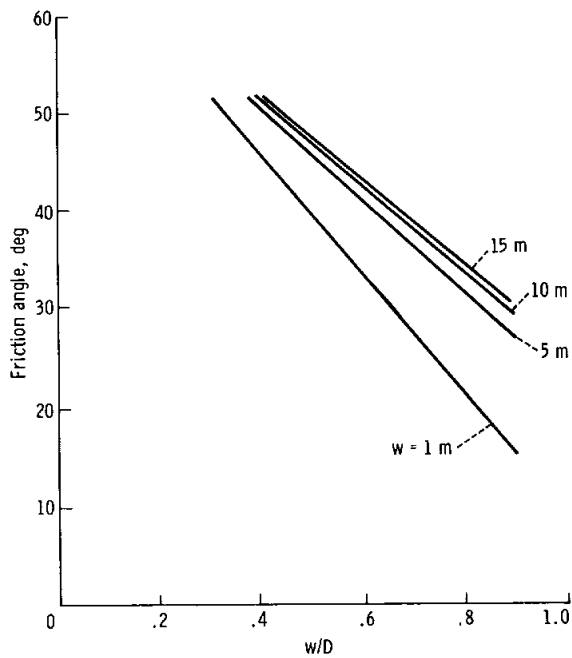
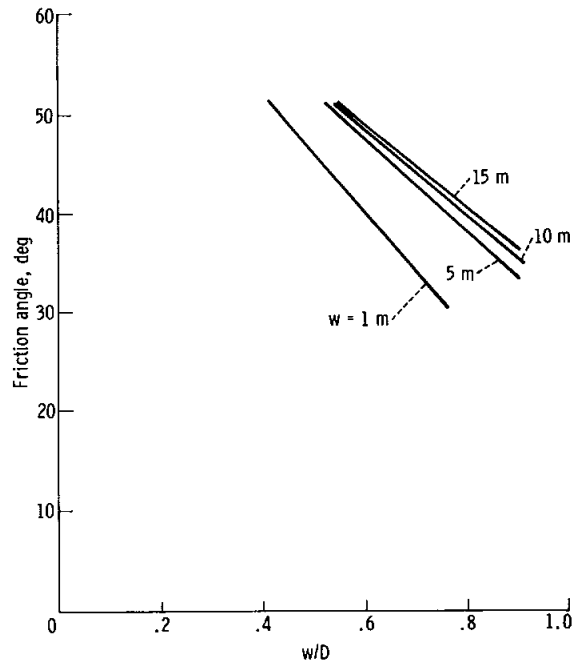
(a) Slope angle = 0° .(c) Slope angle = 20° .(b) Slope angle = 10° .(d) Slope angle = 30° .

FIGURE 8-16.—The relationship between friction angle ϕ and track width to boulder diameter ratio w/D for lunar soil, where soil density ρ_s is 1.6 g/cm^3 ; cohesion c is 1 kN/m^2 ; and rock density/soil density ρ_r/ρ_s is 2.

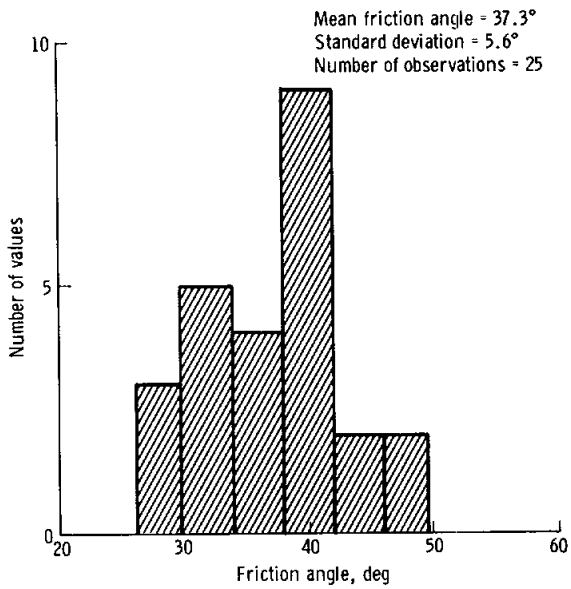


FIGURE 8-17.—Frequency distribution of friction angle values deduced from boulder tracks in the Taurus-Littrow area.

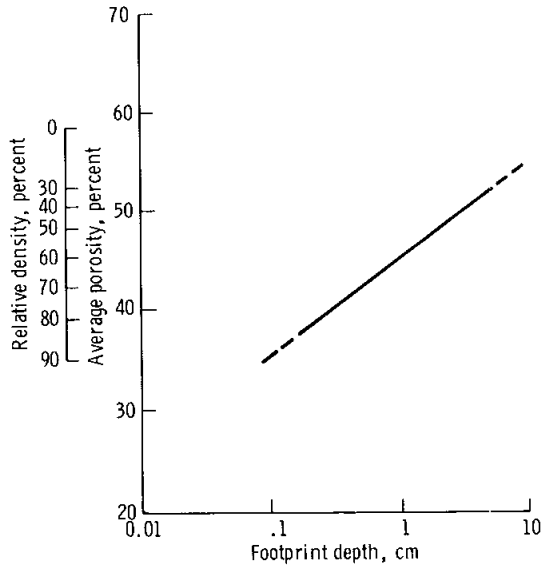


FIGURE 8-18.—Predicted variation of footprint depth with average porosity and relative density in the top 10 cm of the lunar surface. Average porosity is based on a 58.3-percent maximum and a 31-percent minimum. Footprint depth assumes a contact stress of 7 kN/m².

TABLE 8-IV.—Results of Statistical Analysis of Porosities Deduced from Footprint Depths

Location	No. of observations	Mean porosity, ^a percent	Standard deviation	Mean relative density, percent
Apollo 17 site				
All data	144	43.4	2.4	67
LM and ALSEP area	80	43.2	2.65	67
All traverse stations	64	43.65	1.95	66
Intercrater areas				
Apollo 11	30	43.3	1.8	67
Apollo 12	88	42.8	3.1	68
Apollo 14	38	43.3	2.2	67
Apollo 15	117	43.4	2.9	67
Apollo 16	273	45.0	2.8	61.5
Apollo 17	141	43.4	2.4	67
Apollo 11, 12, 14, and 15	273	^b 43.2	^b 2.8	67
All Apollo sites				
Crater rims	89	^b 46.5	^b 4.3	55.5
Intercrater areas	687	^b 44.0	^b 2.75	65
Intercrater areas	687	^c 43.5	^c 2.55	66

^aBased on assumption that n_{max} = 58.3 percent and n_{min} = 31 percent.

^bWeighted average.

^cEach Apollo site given equal weight regardless of number of observations.

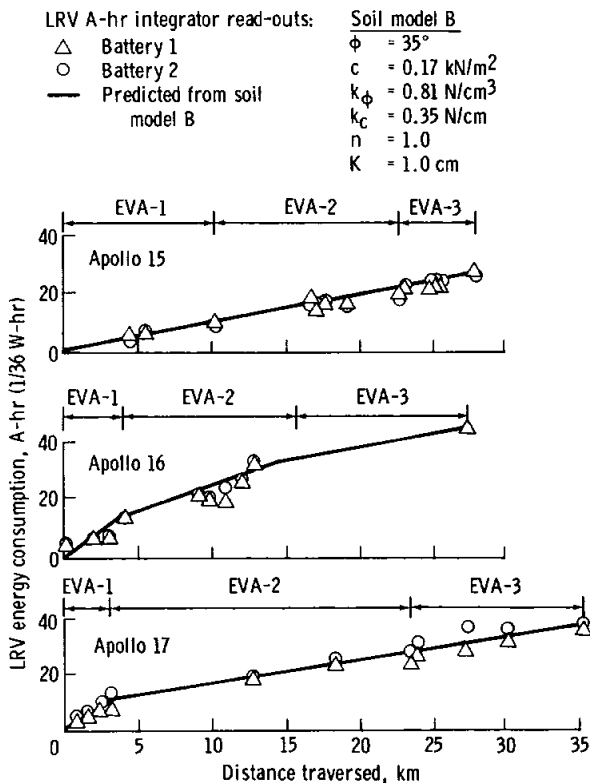


FIGURE 8-21.--Measured energy consumption of the LRV in relation to the predicted values based on the soil properties indicated.

core-tube samples. As shown in figure 8-21, the same soil model, which had been based on Surveyor data for soil near the surface (ref. 8-20), yields results that closely agree with the measured LRV energy consumption at both the Apollo 16 and 17 sites.

In figure 8-21, the symbols ϕ and c designate, respectively, the soil friction angle and cohesion; K is a normalizing constant conditioning the amount of shear strength and the thrust mobilized by the soil at a given wheel slip; and k_ϕ , k_c , and n describe the pressure-sinkage characteristics of the soil under wheel loads (ref. 8-21).

$$p = \frac{k_c}{b} + k_\phi z^n \quad (8-2)$$

in which p is the wheel contact pressure in N/cm^2 , b is the wheel footprint width in centimeters, and z is wheel sinkage in centimeters. If for a given wheel the pressure-sinkage relationship is linear ($n = 1$), the coefficients k_c and k_ϕ are analogous to the penetration resistance gradient of the soil G .

From these parameters, pull as a function of slip and torque as a function of slip relationships were calculated using analytical expressions developed by Bekker (ref. 8-21). These expressions were then used as computer input data, together with other information relating to the mission, terrain, and vehicle characteristics, to calculate the LRV energy consumption at each site (ref. 8-19).

Because of the small amount of wheel sinkage, the LRV wheel/soil interaction with the lunar surface involved predominantly surface shear. Accordingly, a value of $\phi = 35^\circ$ is consistent with average friction angle values deduced from the analysis of LRV tracks (table 8-V) on the basis of in-place plate shear tests performed on a lunar soil simulant (refs. 8-15 and 8-16). The values of coefficients k_c and k_ϕ are consistent with the average G values deduced from LRV tracks (table 8-V). Finally, based on other lunar soil mechanics observations and measurements (e.g., soil erosion during LM descent), an average cohesion value of 0.17 kN/m^2 for the top surficial material was adopted.

In general, the soil/LRV interaction data support the conclusion that the surficial lunar soil is less compact, more deformable and compressible, and has lower strength than does the subsurface material.

Downslope Movements Caused by Meteoroid Impacts

Houston et al. (ref. 8-22) have assessed the relative importance of vibrations induced by meteoroid impact as a mechanism for mass movement of lunar soil downslope. The seismic energy generated by impacts of various-size meteoroids was estimated, and the associated incremental movement was computed for each impact. Movements were summed over the range in meteoroid sizes producing significant movement, both with respect to distance from point of impact and with respect to time, using meteor flux rates derived by Gault (ref. 8-23) with an adjustment based on more recent estimates of the age of the Moon.

The results indicated that the flattest slope on which significant cumulative downslope soil movement of approximately 1 m is likely to have occurred because of impact-produced ground accelerations is approximately 25° . The flattest slope on which cumulative downslope movement of several hundred to a few thousand meters is likely to have occurred is approximately 48° . Because of the great length of

most of the highland lunar slopes, it is estimated that downslope movements of a few thousand meters would be required to cause flattening of the slopes by as much as 1° or 2° . Thus, it appears that only on very steep lunar slopes could there have been significant downslope soil movements caused by shaking from meteoroid impacts alone, and that large-scale slope degradation must have developed primarily by other mechanisms. However, this conclusion does not mean that soil movement, once triggered by meteoroid impact, could not continue as a result of changes in strength properties of the soil mass or fluidization.

Origin of the Light Mantle

It has been hypothesized (ref. 8-24) that the light mantle that extends outward over the plains area north of the base of the South Massif (fig. 8-22) originated as an avalanche from the slopes of the

South Massif. A study of stereographic photographs obtained from orbit during the Apollo 17 mission using the panoramic camera gives some indication of a scarp on the South Massif that could define the boundary of a slide mass. Furthermore, according to the LSPET, the light mantle material on the plains appears to be compositionally similar to that from the South Massif. Thus, reasonable evidence exists that a slide or avalanche did occur. If a slide did occur, then an important question to be resolved is the mechanism by which the material spread out onto the valley floor and came to rest with a nearly level surface.

As the slope of the South Massif is only approximately 25° to 30° , meteoroid impact is unlikely to have been able to do much more than just initiate movement. Incremental movements accumulating from impacts alone could not account for the magnitude of movements indicated. However, once a

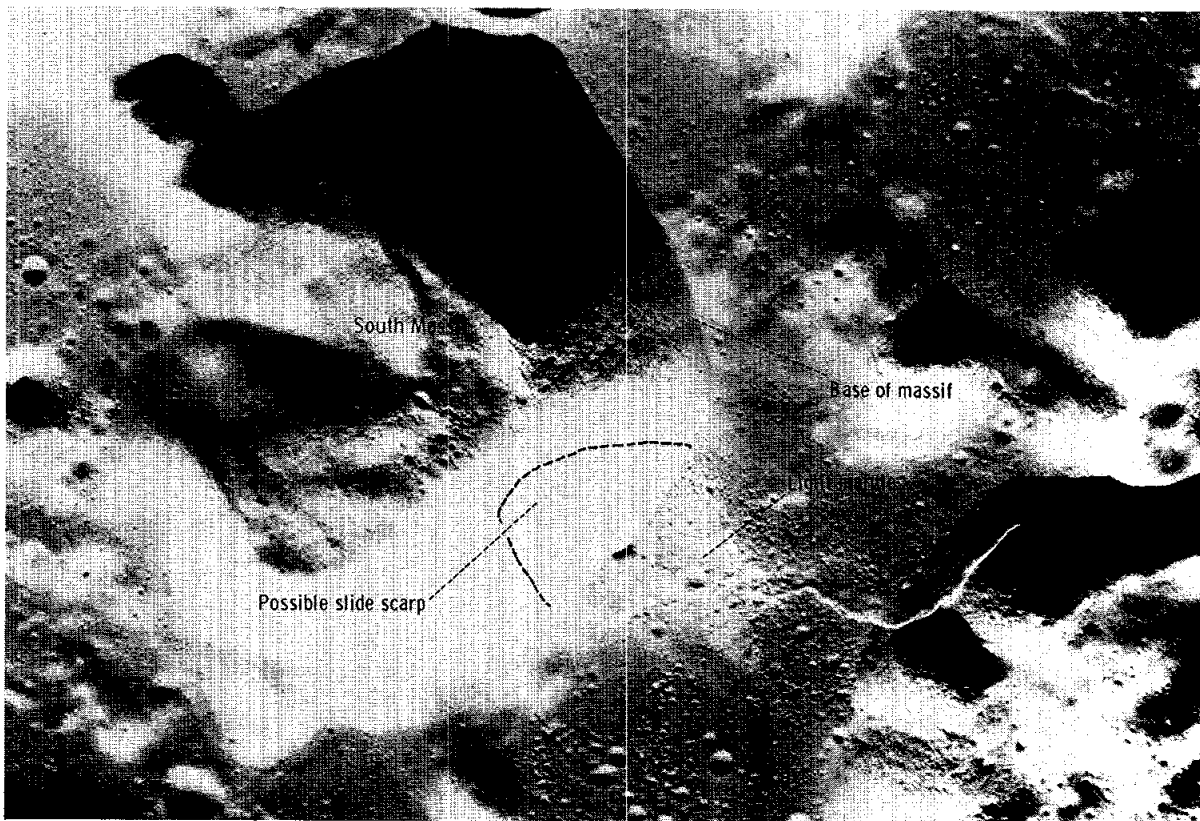


FIGURE 8-22.—Orbital view of the Apollo 17 landing area. The light mantle to the north of the South Massif may have been an avalanche produced by the mechanisms proposed in text. A possible slide scarp can be seen located as indicated on high-resolution panoramic camera photographs (Apollo 17 panoramic camera frame AS17-2314).

slide was triggered, if the soil strength were to decrease significantly or if the mass became fluidized because of the generation or liberation of significant quantities of gas, then continued movement might be possible.

In the analysis of downslope movements referred to previously, no change in soil strength was assumed once failure occurred. The nature of lunar soil particles, particularly the agglutinates and breccias, is such that particle breakdown during shear is likely. The results of strength and compression tests on lunar soil samples by Carrier et al. (ref. 8-25) suggest that particle breakdown does indeed occur. Mitchell and Houston (ref. 8-26) found that decreasing the particle size of a basalt lunar soil simulant resulted in a significant decrease in the angle of internal friction. It is not likely, however, that particle comminution could lead to a decrease in friction angle to a value less than 25° , which would be required to result in any slope flattening on the South Massif. A loss in strength caused by a friction-angle decrease sufficient to allow spreading of the material over the level plains does not seem possible.

The plausibility of fluidization as a mechanism hinges on the generation or liberation of sufficient gas during the initial stages of movement to provide a sufficient uplift pressure on the overlying soil to reduce or eliminate frictional resistance to downslope movement. Gas of solar wind origin was liberated in the compression and strength tests described in reference 8-24; however, the amount was too small by orders of magnitude to cause fluidization. Conversely, other investigators have generated gas by a combination of grinding and heating.

Clanton et al. (ref. 8-27) and Bogard et al. (ref. 8-28) have confirmed that agglutinates are enriched in solar wind and thus could serve as a source of gas when broken down. The Apollo 17 soil composition analyses indicate that the samples from the massifs contain greater proportions of breccias, approximately the same proportion of agglutinates, and less basalt than does the dark mantle material on the plains. Thus, a fluidization mechanism may be tenable to account for the origin of the light mantle, whereas fluidization would be very unlikely if the massifs were composed only of ground-up basalt.

CONCLUSIONS

The physical and mechanical properties of the soil at the Apollo 17 landing site are generally similar to

those of the soils at the previous Apollo sites. Although no crew tasks or lunar surface measurements were done specifically for the purpose of obtaining quantitative soil mechanics data, a number of preliminary analyses and interpretations have been made using EVA transcripts and kinescopes, photographs, data on soil/LRV interactions, debriefings, and limited examination of returned lunar samples. The following specific conclusions have been developed.

1. Soil cover is present at all points visited in the Taurus-Littrow landing area. Surface textures and colors are similar to those at the other Apollo sites.

2. There is considerable local (meter scale) variability in soil properties.

3. Particle-size distributions of samples from different traverse stations are generally similar to each other and to those observed at previous landing sites, even though soil compositions are highly variable among the stations in terms of proportions of basalt, breccia, mineral fragments, glass, and agglutinates.

4. The drive-tube samples indicate some increase in density with depth but more uniformity with depth than the Apollo 15 and 16 samples. Soil density in the double drive tube taken on the rim of Shorty Crater (station 4) is higher than heretofore observed for any lunar sample. The presence of high specific gravity particles, such as ilmenite, is a more probable cause than is very low porosity.

5. Absolute densities at the Apollo 17 drill site are generally higher than those measured at the Apollo 15 and 16 drill sites, and the distribution of densities with depth suggests a different depositional history from that at the previous two sites.

6. Stability analysis of the open drill-stem hole, into which the neutron flux probe was placed and removed without soil resistance, indicates that there was little or no squeezing or caving of the soil during a 49-hr period and that soil strength at a depth of 2 m must have been considerably greater than the average strength near the surface.

7. Tracks caused by the rolling and bouncing of boulders are common on the slopes of the massifs and the Sculptured Hills. A frequency distribution of soil friction angles was deduced from rolling boulder track data that is consistent with the soil gradations, densities, and porosities found at other locations on the Moon, although the absolute values of friction angle were computed to be somewhat lower than was anticipated.

8. Near-surface soil porosities deduced from foot-

print depths indicate that neither the intercrater average porosity nor the standard deviation differ significantly from the average values for previous Apollo sites. The average relative density for all Apollo landing sites, as deduced from 687 observations of footprint depth, is approximately 66 percent. Large local (meter scale) variations exist in porosity and relative density.

9. The LRV performance, including slope-climbing capability and power consumption, was within the predicted limits. Analysis of track depth, shape, and texture indicated no discernible variations in the average consistency of the surface soil throughout the Taurus-Littrow region or relative to the Apollo 14 through 17 and Luna 17 landing sites, although variations about the average existed on a small scale at all sites.

10. Only on very steep lunar slopes ($> 25^\circ$) could there have been significant downslope soil movements caused by shaking from meteoroid impacts alone, and large-scale slope degradation must have developed primarily by other mechanisms.

11. There is evidence to support an avalanche as the origin of the light mantle covering the plains north of the South Massif. Fluidization of the soil mass by gas pressures generated during the initial phases of soil movement would be required to account for the large-scale movements observed.

Finally, soil mechanics data from all the Apollo missions support the general conclusion that processes affecting the entire lunar surface, such as meteoroid impact and the solar wind, control the average properties such as grain-size distribution and relative density, which are nearly the same at all sites. On the average, the soil on slopes is less dense than the soil on level areas because of the effects of downslope movement. Local geology and topography on a small scale and specific cratering events appear to control the variations about the average to the extent that the standard deviation can be relatively large.

REFERENCES

- 8-1. Mitchell, J. K.; Houston, W. N.; Scott, R. F.; Costes, N. C.; et al.: Mechanical Properties of Lunar Soil: Density, Porosity, Cohesion, and Angle of Internal Friction. Proceedings of the Third Lunar Science Conference, vol. 3, MIT Press (Cambridge, Mass.), 1972, pp. 3235-3253.
- 8-2. Carrier, W. D., III; Mitchell, J. K.; and Mahmood, Arshud: The Relative Density of Lunar Soil. Lunar Science IV (Abs. of papers presented at the Fourth Lunar Science Conference (Houston, Tex.), Mar. 5-8, 1973), pp. 118-120.
- 8-3. Houston, W. N.; Hovland, H. J.; and Mitchell, J. K.: Lunar Soil Porosity and Its Variation as Estimated from Footprints and Boulder Tracks. Proceedings of the Third Lunar Science Conference, vol. 3, MIT Press (Cambridge, Mass.), 1972, pp. 3255-3263.
- 8-4. Mitchell, J. K.; Carrier, W. D., III; Houston, W. N.; Scott, R. F.; et al.: Soil Mechanics. Sec. 8 of the Apollo 16 Preliminary Science Report. NASA SP-315, 1972.
- 8-5. Costes, N. C.: Regional Variations in Physical and Mechanical Properties of Lunar Surface Regolith. Lunar Science IV (Abs. of papers presented at the Fourth Lunar Science Conference (Houston, Tex.), Mar. 5-8, 1973), pp. 159-161.
- 8-6. Hovland, H. J.; and Mitchell, J. K.: Mechanics of Rolling Sphere-Soil Slope Interaction. Final Rept. (NASA Contract NAS 8-21432), Vol. II, Space Sci. Lab., Univ. of California at Berkeley, July 1971.
- 8-7. Carrier, W. D., III: Lunar Soil Grain Size Distribution. The Moon, vol. 8, 1973.
- 8-8. Mitchell, J. K.; Bromwell, L. G.; Carrier, W. D., III; Costes, N. C.; et al.: Soil-Mechanics Experiment. Sec. 7 of the Apollo 15 Preliminary Science Report. NASA SP-289, 1972.
- 8-9. Grolier, M. J.; Moore, H. J.; and Martin, G. L.: Lunar Block Tracks. A Preliminary Geologic Evaluation of Areas Photographed by Lunar-Orbiter V Including an Apollo Landing Analysis of One of the Areas. NASA Langley Research Center, Rept. LWP-506, 1968, pp. 143-154.
- 8-10. Filice, A. L.: Lunar Surface Strength Estimate from Orbiter II Photographs. Science, vol. 156, no. 3781, June 16, 1967, pp. 1486-1487.
- 8-11. Eggleston, J. M.; Patterson, A. W.; Throop, J. E.; Arant, W. H.; and Spooner, D. L.: Lunar Rolling Stones. Photogrammetric Eng., vol. 34, no. 3, Mar. 1968, pp. 246-255.
- 8-12. Moore, H. J.: Estimates of the Mechanical Properties of Lunar Surface Using Tracks and Secondary Impact Craters Produced by Blocks and Boulders. U.S. Geol. Survey Interagency Rept.: Astrogeology 22, July 1970.
- 8-13. Moore, H. J.; Vischer, W. A.; and Martin, G. L.: Boulder Tracks on the Moon and Earth. U.S. Geol. Survey Prof. Paper 800-B, 1972, pp. B165-B174.
- 8-14. Houston, W. N.; and Namiq, L. I.: Penetration Resistance of Lunar Soils. J. Terramechanics, vol. 8, no. 1, 1971, pp. 59-69.
- 8-15. Green, A. J.; and Melzer, K. J.: Performance of the Boeing LRV Wheels in a Lunar Soil Simulant: Effect of Wheel Design and Soil. Tech. Rept. M-71-10, Rept. 1, USAE WES, Vicksburg, Miss., 1971.
- 8-16. Melzer, K. J.: Performance of the Boeing LRV Wheels in a Lunar Soil Simulant: Effect of Speed, Wheel Load, and Soil. Tech. Rept. M-71-10, Rept. 2, USAE WES, Vicksburg, Miss., 1971.
- 8-17. Vinogradov, A. P., ed.: Lunokhod-1, Mobile Lunar Laboratory. Nanka Publishers (Moscow), 1971. (Available from National Technical Information Service, Springfield, Virginia.)
- 8-18. Mitchell, J. K.; Bromwell, L. G.; Carrier, W. D., III; Costes, N. C.; and Scott, R. F.: Soil Mechanical Properties

- at the Apollo 14 Site. *J. Geophys. Res.*, vol. 77, no. 29, Oct. 10, 1972, pp. 5641-5664.
- 8-19. Costes, N. C.; Farmer, J. E.; and George, E. B.: Mobility Performance of the Lunar Roving Vehicle. *Terrestrial Studies: Apollo 15 Results*. NASA TR R-401, 1972.
- 8-20. Scott, R. F.; and Roberson, F. I.: Soil Mechanics Surface Sampler. Part II: Surveyor Project Final Report, Calif. Inst. Tech. JPL-TR-32-1265, 1968, pp. 195-207.
- 8-21. Bekker, M. G.: *Introduction to Terrain-Vehicle Systems*. The University of Michigan Press (Ann Arbor, Mich.), 1969.
- 8-22. Houston, W. N.; Moriwaki, Y.; and Chang, C. S.: Downslope Movement of Lunar Soil and Rock Caused by Meteor Impact. *Lunar Science IV* (Abs. of papers presented at the Fourth Lunar Science Conference (Houston, Tex.), Mar. 5-8, 1973), pp. 384-385.
- 8-23. Gault, D. E.: Saturation and Equilibrium Conditions for Impact Cratering on the Lunar Surface: Criteria and Implications. *Radio Sci.*, vol. 5, no. 2, Feb. 1970, pp. 273-291.
- 8-24. Howard, K. A.: Lunar Avalanches. *Lunar Science IV* (Abs. of papers presented at the Fourth Lunar Science Conference (Houston, Tex.), Mar. 5-8, 1973), pp. 386-388.
- 8-25. Carrier, W. D., III; Bromwell, L. G.; and Martin, R. T.: Behavior of Returned Lunar Soil in Vacuum. *J. Soil Mechanics Foundations Div., ASCE*, Nov. 1973.
- 8-26. Mitchell, J. K.; and Houston, W. N.: Lunar Surface Engineering Properties Experiment Definition. Final Rept., Vol. 1 (NASA CR-102963), Space Sci. Lab., Univ. of California at Berkeley, 1970.
- 8-27. Clanton, U. S.; McKay, D. S.; Taylor, R. M.; and Heiken, G. H.: Relationship of Exposure Age to Size Distribution and Particle Types in the Apollo 15 Drill Core. *The Apollo 15 Lunar Samples*, Lunar Science Institute (Houston, Tex.), 1972, pp. 54-56.
- 8-28. Bogard, D. D.; Nyquist, L. E.; Hirsch, W. C.; and Moore, D. R.: Trapped Noble Gas Abundances in Surface and Sub-Surface Fines From Apollo 15 and 16. *Lunar Science IV* (Abs. of papers presented at the Fourth Lunar Science Conference (Houston, Tex.), Mar. 5-8, 1973), pp. 79-81.